THE JOURNAL OF BIOLOGICAL CHEMISTRY VOL. 281, NO. 35, pp. 25297–25306, September 1, 2006

Biochemical Basis of Genotoxicity of Heterocyclic Arylamine Food Mutagens

HUMAN DNA POLYMERASE η SELECTIVELY PRODUCES A TWO-BASE DELETION IN COPYING THE N^2-GUANYL ADDUCT OF 2-AMINO-3-METHYLIMIDAZO[4,5-f]QUINOLINE BUT NOT THE C^8 ADDUCT AT THE NarI G3 SITE[S]*

Received for publication, June 14, 2006, and in revised form, July 7, 2006 Published, JBC Papers in Press, July 10, 2006, DOI 10.1074/jbc.M605699200

Jeong-Yun Choi[‡§¶], James S. Stover[§‖], Karen C. Angel[‡§], Goutam Chowdhury[‡§1], Carmelo J. Rizzo[§‖], and F. Peter Guengerich[‡§2]

From the Departments of [‡]Biochemistry and [‖]Chemistry and the [§]Center in Molecular Toxicology, Vanderbilt University, Nashville, Tennessee 37232-0146 and the [¶]Department of Pharmacology, Ewha Womans University, Seoul 158-710, Republic of Korea

Heterocyclic arylamines are highly mutagenic and cause tumors in animal models. The mutagenicity is attributed to the C^8- and N^2-G adducts, the latter of which accumulates due to slower repair. The C^8- and N^2-G adducts derived from 2-amino-3-methylimidazo[4,5-*f*]quinoline (IQ) were placed at the G_1 and G_3 sites of the NarI sequence, in which the G_3 site is an established hot spot for frameshift mutation with the model arylamine derivative 2-acetylaminofluorene but G_1 is not. Human DNA polymerase (pol) η extended primers beyond template G-IQ adducts better than did pol κ and much better than pol ι or δ. In 1-base incorporation studies, pol η inserted C and A, pol ι inserted T, and pol κ inserted G. Steady-state kinetic parameters were measured for these dNTPs opposite the C^8- and N^2-IQ adducts at both sites, being most favorable for pol η. Mass spectrometry of pol η extension products revealed a single major product in each of four cases; with the G_1 and G_3 C^8-IQ adducts, incorporation was largely error-free. With the G_3 N^2-IQ adduct, a −2 deletion occurred at the site of the adduct. With the G_1 N^2-IQ adduct, the product was error-free at the site opposite the base and then stalled. Thus, the pol η products yielded frameshifts with the N^2 but not the C^8 IQ adducts. We show a role for pol η and the complexity of different chemical adducts of IQ, DNA position, and DNA polymerases.

The modification of DNA by chemical and physical agents is a common process and leads to loss of genetic stability (1), a factor in aging, cancer, and various other maladies, *e.g.* cardiovascular disease (2). Therefore, questions about the chemistry of the damage and the biochemical processing are of particular interest regarding many diseases, as well as basic molecular genetics (1). Repair of DNA damage is one issue, but another issue is the replication of damaged DNA and the introduction of mutations (1, 3). The field has become more complex with the discovery of a plethora of translesion DNA polymerases, some of which appear to have selective functions in replicating damaged DNA (1, 4). Today at least 14 human DNA polymerases are known (1, 5), and defining roles of individual polymerases in complex processes is an area of considerable interest (3, 5, 6). A major general issue is the elucidation of the bases for the selectivity of chemical and physical agents in producing various mutation spectra in individual genes, ultimately a factor in biological outcomes. Several contributors are as follows: (i) reaction of the chemical or physical agent with DNA; (ii) further nonenzymatic reactions of the DNA adduct; (iii) DNA repair (or lack of repair); (iv) the action of DNA polymerases; and (v) the biological effect of a particular mutation in changing the phenotype (3, 7).

Heterocyclic amines are an important class of chemical carcinogens (8–10). A number of these compounds are produced by pyrolysis of food and tobacco (10–12) and were originally identified on the basis of their extremely strong mutagenic properties in bacteria (8, 13). The heterocyclic amines have chemical (and biochemical) similarity to arylamines, several of which are recognized human carcinogens (14, 15). Several heterocyclic amines have been shown to be carcinogenic in rodents and non-human primates (16).

Arylamines and the derivative arylacetamides can show strong sequence selectivity in mutational assays. For example, in bacterial systems on adducts derived from AAF,[3] a strong −2

* This work was supported in part by United States Public Health Service Grants R01 ES010375 (to F. P. G.), T32 ES007028 (to J. S. S.), and P30 ES000267 (to F. P. G. and C. J. R.). The costs of publication of this article were defrayed in part by the payment of page charges. This article must therefore be hereby marked "*advertisement*" in accordance with 18 U.S.C. Section 1734 solely to indicate this fact.

[S] The on-line version of this article (available at http://www.jbc.org) contains Figs. S1–S8 and the characterization of the four modified template oligonucleotides (CGE and MS), MS of synthesized 5′-pGGCGCCGAGT-3′ used to confirm the assignment of the product identified in the primer extension opposite the C^8-IQ adduct at the G_3 template site (Fig. 5 of text), analysis of the pol η extension products of the primer extended opposite the template containing the C^8-IQ and N^2-IQ adducts at the G_1 site using LC-MS/MS, and analysis of the possible extension beyond a G_1 site N^2-IQ G:A pair by pol η.

[1] Supported in part by a Merck fellowship.

[2] To whom correspondence should be addressed: Dept. of Biochemistry and Center in Molecular Toxicology, Vanderbilt University School of Medicine, 638 Robinson Research Bldg., 23rd and Pierce Aves., Nashville, TN 37232-0146. Tel.: 615-322-2261; Fax: 615-322-3141; E-mail: f.guengerich@vanderbilt.edu.

[3] The abbreviations used are: AAF, 2-acetylaminofluorene; AF, 2-aminofluorene; CGE, capillary gel electrophoresis; CID, collision-induced dissociation; ES, electrospray; IQ, 2-amino-3-methylimidazo[4,5-*f*]quinoline; LC, (high performance) liquid chromatography; MALDI-TOF, matrix-assisted laser desorption/time-of-flight; MS, mass spectrometry; PCNA, proliferating cell nuclear antigen; pol, DNA polymerase; UDG, uracil DNA glycosylase; HPLC, high pressure liquid chromatography.

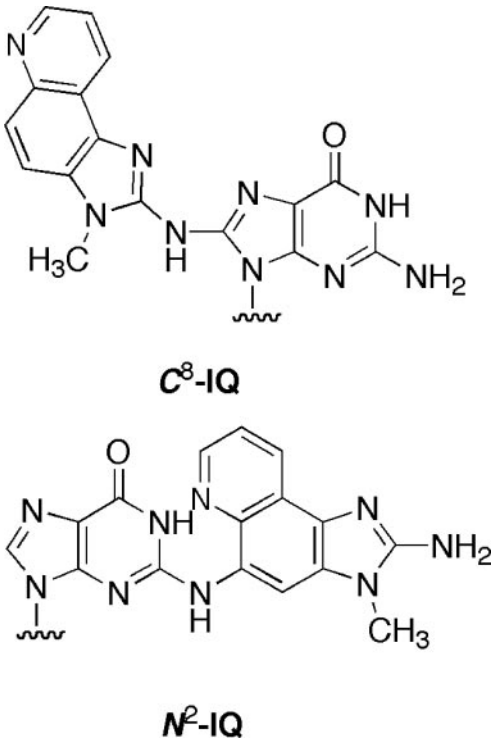

FIGURE 1. **Guanine N^2- and C^8 adducts of IQ.**

frameshift (deletion) is seen at the "G_3" site of the NarI sequence (GGCGCC), leading to the loss of a GC doublet (17–19). This phenomenon, which is not observed with the closely related compound AF, has been studied at several structural and biological levels (20–22). The basis is more complex than alteration of the DNA structure, in that not only the site within the DNA but also the cellular system influences the biological outcome (23). The NarI "hot spot" was first detected in analysis of the mutation spectrum or AAF (17); repetitive sequences have been detected as being prone to frameshift mutagenesis with various systems (18, 19). The position of the adduct within the repetitive NarI sequence has a strong effect on whether mutations occur or not, as shown with AAF (19).

One of the critical issues in the study of the biochemical mechanisms of processing of DNA damage is the ability to prepare specific chemical reagents, particularly DNA adducts. Using methods developed in our laboratories, we have been able to avoid producing mixtures of heterocyclic amine DNA adducts with the use of strategies for synthesis of appropriately modified monomers (24–26). With this strategy, we were able to synthesize both of the major DNA adducts formed by IQ, the N^2- and C^8-guanyl adducts (Fig. 1). Both of these adducts are formed upon reaction of DNA with *N*-hydroxy IQ (27), but the proportion of the N^2-IQ adduct increases with time *in vivo* (in rodents) due to much slower repair (27, 28). Both adducts were positioned at both the G_1 and the G_3 sites in the NarI sequence, which are known to be resistant and sensitive, respectively, to frameshift mutations with AAF (19, 29). The modified oligonucleotides were used in studies with purified recombinant human DNA polymerases, including the replicative pol δ-PCNA complex and the major translesion polymerases pol η, ι, and κ. Analysis included primer extension in the presence of all four dNTPs, steady-state kinetic analysis of single dNTP insertion, and LC-MS/MS sequencing analysis of the full-length extension products. The results show that pol δ is completely blocked by the IQ adducts and that pol η is the most efficient of the translesion DNA polymerases in copying. pol η exhibited different behavior with both of the two IQ adducts at each of the two internal NarI sites. In particular, the N^2-IQ adduct (with pol η) yielded only the −2 deletion product at the G_3 site, which was not observed with the C^8-IQ adduct. The selectivity of pol η for the site-specific lesions is striking and correlates not only to the NarI G_3 frameshift seen in bacteria but also a prominent GC deletion seen in several tissues of rats treated with IQ (30).

EXPERIMENTAL PROCEDURES

Enzymes—Recombinant human pol δ (4-subunit mixture) (31), pol η (31), pol ι (32), and pol κ (33) were (individually) expressed in baculovirus-infected insect cell systems and purified as described previously. Recombinant human PCNA was prepared in *Escherichia coli* and purified as described elsewhere (34, 35).

Oligonucleotide Synthesis—The adducted oligonucleotides (24–26) were synthesized on an Expedite 8909 DNA synthesizer (PerSeptive Biosystems) on a 1-μmol scale using the UltraMild line of phosphoramidites (phenoxyacetyl-protected dA, 4-isopropyl-phenoxyacetyl-protected dG, acetyl-protected dC, and dT phosphoramidites) and solid supports from Glen Research (Sterling, VA) (Table 1). The manufacturer's standard synthesis protocol was followed except at the incorporation of the modified phosphoramidites, which was accomplished manually, off-line. At this point, the column was removed from the instrument and sealed with two syringes, one of which contained 250–300 μl of the manufacturer's 1*H*-tetrazole activator solution (1.9–4.0% in CH_3CN, w/v) and the other contained 250 μl of the phosphoramidite (15 mg, 98 mM in anhydrous CH_2Cl_2). The 1*H*-tetrazole and the phosphoramidite solutions were sequentially drawn through the column (1*H*-tetrazole first), and this procedure was repeated periodically over 30 min. After this time, the column was washed with manufacturer's grade anhydrous CH_3CN and returned to the instrument for the capping, oxidation, and detritylation steps. The remainder of the synthesis was carried out in the usual manner.

HPLC—HPLC analyses and purifications were performed on a Beckman HPLC system with a UV diode array detector (model 166) monitored at 254 nm and utilizing 32 Karat software (version 3.1). The oligonucleotides were purified by using a 20 mM sodium phosphate buffer (pH 7.0, solvent 1) and CH_3OH (solvent 2). The solvent gradient was as follows: initially 99% solvent 1 (v/v), then a 27.5-min linear gradient to 35% solvent 1 (v/v); a 2.5-min linear gradient to 50% solvent 1 (v/v) followed by 5-min isocratic at 50% solvent 1 (v/v), and then a 5-min linear gradient to initial conditions.

CGE—Electrophoretic analyses were carried out using a Beckman P/ACE Instrument System 5500 Series system, monitored at 260 nm. The P/ACE MDQ instrument used a 31.2 cm × 100 μm eCAP capillary with samples applied at 10 kV and

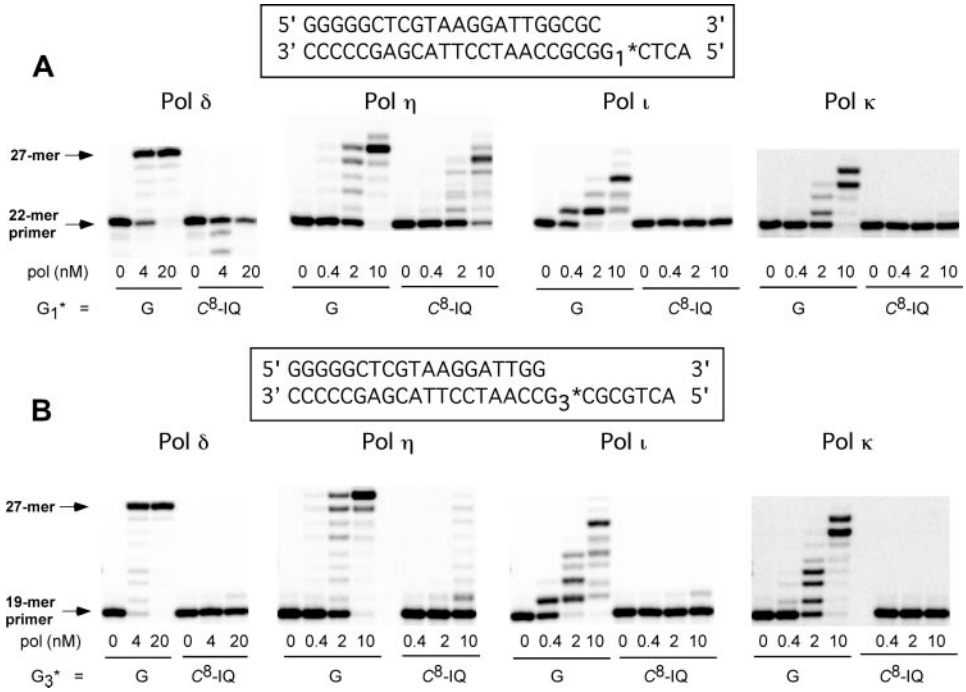

FIGURE 2. **Extension of ^{32}P-labeled primer paired with a 27-mer template containing G or C^8-IQ G.** *A*, ^{32}P-labeled 22-mer was annealed with a 27-mer containing G or C^8-IQ G at position 23 (G_1). *B*, ^{32}P-labeled 19-mer was annealed with a 27-mer containing G or C^8-IQ G at position 20 (G_3). All incubations were done for 15 min with 100 nM primer-template and the indicated concentration of the polymerase in the presence of all four dNTPs. PCNA (400 nM) was present in the case of pol δ. The lengths of the bands are indicated.

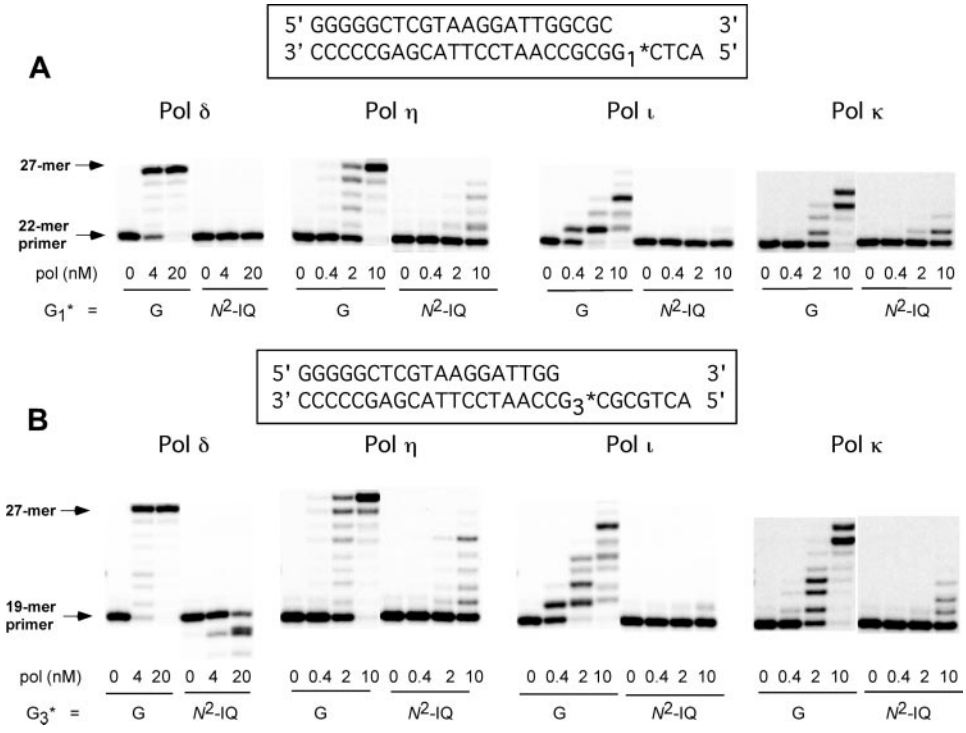

FIGURE 3. **Extension of ^{32}P-labeled primer paired with a 27-mer template containing G or N^2-IQ G.** *A*, ^{32}P-labeled 22-mer was annealed with a 27-mer containing G or N^2-IQ G at position 23 (G_1). *B*, ^{32}P-labeled 19-mer was annealed with a 27-mer containing G or N^2-IQ G at position 20 (G_3). All incubations were done for 15 min with 100 nM primer-template and the indicated concentration of the polymerase in the presence of all four dNTPs. PCNA (400 nM) was present in the case of pol δ. The lengths of the bands are indicated.

run at 9 kV. The column was packed with the manufacturer's 100-R gel (for single-stranded DNA) using a Tris borate buffer system containing 7.0 M urea. CGE electrophoretograms of all modified oligonucleotides are presented in supplemental Figs. S1–S4.

MALDI-TOF Sequencing of Oligonucleotides—MALDI-TOF mass spectra of the four intact IG-containing templates are presented in supplemental Figs. S1–S4.

MALDI-TOF MS sequencing of modified oligonucleotides (36) was performed by treatment of purified oligonucleotides (0.3 A_{260} units, based on 1-ml volume) in an ammonium hydrogen citrate buffer (pH 9.4) with 2 milliunits of phosphodiesterase I. Aliquots of 4 μl were taken before enzyme addition and at 1-, 8-, 18-, 28-, and 38-min time points and added sequentially to the same vial, which was kept frozen on dry ice. A second DNA aliquot (0.3 A_{260} units in 24 μl of 20 mM ammonium acetate (pH 6.6)) was treated with 2 milliunits of phosphodiesterase II, and aliquots of 4 μl were taken in the same manner. The two digest mixtures were desalted using Millipore C_{18} Ziptips and eluted directly onto a MALDI plate in 3-hydroxypicolinic acid-containing ammonium hydrogen citrate (7 mg ml^{-1}). MALDI-TOF analysis allowed sequential identification of nucleotides from the 3′ end of the sequence for the phosphodiesterase I-treated sample and from the 5′ end for the phosphodiesterase II-treated sample. Both phosphodiesterase treatments confirmed the expected positions of the G_1 and G_3 site adducts in the synthetic templates containing C^8- and N^2-IQ (data not presented).

Reaction Conditions for Enzyme Assays—Unless indicated otherwise, standard DNA polymerase reactions were done in 50 mM Tris-HCl buffer (pH 7.5) containing 5 mM dithiothreitol, 100 μg of bovine serum albumin ml^{-1} (w/v), and 10% glycerol (v/v) with 100 nM primer-template at 37 °C. Primers (19- or 22-mer) were 5′ end-labeled using T4 polynucleotide kinase/[γ-^{32}P]ATP and annealed with templates (27-mers). All reactions were initiated by the addition of dNTP solutions containing $MgCl_2$ (5 mM final concentration) to preincubated enzyme/DNA mixtures.

Primer Extension Assay with All Four dNTPs ("Run-on" or "Standing Start" Experiments)—A ^{32}P-labeled primer, annealed to either an unmodified or modified (N^2-IQ G or C^8-IQ G) template, was extended in the presence of all four dNTPs (100 μM each) for 15 min. Reaction mixtures (8 μl) were quenched with 10 volumes of a solution of 20 mM EDTA in 95% formamide (v/v). Products were resolved using a 16% (w/v) PAGE system containing 8 M urea and visualized using a Molecular Imager (model FX) and Quantity One software (Bio-Rad).

Steady-state Kinetic Analyses—A ^{32}P-labeled primer, annealed to either an unmodified or adducted template, was extended in the presence of varying concentrations of a single dNTP. The molar ratio of primer-template complex to enzyme was at least 10:1, except for the adducted templates with pol κ and pol ι (molar ratio of 5–30:1). Polymerase concentrations and reaction times were chosen so that maximal product formation was ≤20% of the substrate concentration. The reactions with the modified oligonucleotides were relatively slow, as shown with the results (which are typical for studies in this field). The primer-template complex was extended with each dNTP in the presence of 0.1–20 nM enzyme for 10 min. All reactions (8 μl, done at 10 dNTP concentrations) were quenched with 10 volumes of a solution of 20 mM EDTA in 95% formamide (v/v). Products were resolved using a 16% polyacrylamide (w/v) electrophoresis gel containing 8 M urea and quantitated with PhosphorImaging analysis using a Molecular Imager FX instrument and Quantity One software (Bio-Rad). Graphs of product formation *versus* dNTP concentration were fit using nonlinear regression (hyperbolic fits) in GraphPad Prism version 3.0 (GraphPad, San Diego) for the estimation of k_{cat} and K_m values.

LC-MS/MS Analysis of Oligonucleotide Products from pol η Reactions—pol η reactions were performed for 6 h at 37 °C in 50 mM Tris-HCl (pH 7.8) buffer containing 1 mM dithiothreitol, 50 μg of bovine serum albumin ml^{-1}, 50 mM NaCl, and 5 mM $MgCl_2$ (200 μl total reaction mixture). The reactions were done with all four dNTPs at 1 mM each, 5 μM oligonucleotide substrate, and pol η concentrations of 1.25–2.5 μM. The reactions were terminated by extracting the dNTPs using a spin column (Bio-Spin 6, Bio-Rad). The initial concentrations of Tris-HCl, EDTA, and dithiothreitol were restored in the above filtrate, and 15 units of *E. coli* UDG was added to the mixtures. The reactions were allowed to incubate at 37 °C for 4 h. Piperidine was added to the reaction mixtures (to 0.25 M), which were heated at 95 °C for 1 h followed by lyophilization. The residues were dissolved in a 70-μl volume for LC-MS/MS analysis.

For most of the experiments, MS analysis was performed in the Vanderbilt facility on a DecaXP ion trap instrument (ThermoFinnigan, San Jose, CA), using the general methods described earlier (37, 38). Samples were injected using an autosampler, with 10 μl withdrawn from the reaction mixture. The mixtures were separated on a Jupiter microbore column (1.0 mm × 150 mm, 5 μm; Phenomenex, Torrance, CA). Buffer A contained 10 mM $NH_4CH_3CO_2$ (pH 6.8) and 2% CH_3CN (v/v). Buffer B contained 10 mM $NH_4CH_3CO_2$ (pH 6.8) and 98% CH_3CN (v/v). The flow rate was 1.0 ml min^{-1}, and the gradient was as follows: 0–2 min, hold at 100% A; 2–20 min, linear program to 100% B; 20–30 min, hold at 100% B; 30–32 min, linear program to 100% A; 32–40 min, hold at 100% A (for next injection). Oligonucleotides eluted at t_R 9–12 min. Electrospray conditions (negative ion) were as follows: source voltage 3.4 kV, source current 8.5 μA, sheath gas flow rate setting 28.2, auxiliary sweep gas flow rate setting 4.3, capillary voltage 49 V, capillary temperature 230 °C, tube lens voltage 67 V. MS/MS settings were as follows: normalized collision energy 35%, activation Q 0.250, time 30 min, 1 scan. Product ion spectra were acquired over the range *m/z* 300–2000. The most abundant ions were selected for CID analysis. The calculations of the CID fragmentations of a certain oligonucleotide sequence were done using a program from the Mass Spectrometry Group of Medicinal Chemistry at the University of Utah.

TABLE 1
Oligonucleotides used in this study
G* indicates G, C^8-IQ G, or N^2-IQ G.

19-mer	5′-GGGGGCTCGTAAGGATTGG
22-mer	5′-GGGGGCTCGTAAGGATTGGCGC
27-mer	3′-CCCCCGAGCATTCCTAACC**G$_3$***CG$_2$**G$_1$***CTCA

TABLE 2
Steady-state kinetic parameters for 1-base incorporation opposite G_1 by human pol η, ι, and κ

Polymerase	Template	dNTP	K_m	k_{cat}	k_{cat}/K_m	f (misinsertion frequency)
			μM	s^{-1}	$mM^{-1}\ s^{-1}$	
pol η	dG_1	C	1.7 ± 0.2	0.12 ± 0.004	71	1
		A	240 ± 50	0.037 ± 0.002	0.15	0.0021
	dG_1-C^8-IQ	C	19 ± 2	0.18 ± 0.004	9.5	1
		A	120 ± 10	0.011 ± 0.0003	0.092	0.0097
	dG_1-N^2-IQ	C	42 ± 6	0.028 ± 0.001	0.68	1
		A	85 ± 10	0.041 ± 0.001	0.48	0.71
pol ι	dG_1	C	99 ± 11	0.33 ± 0.01	3.3	1
		T	220 ± 40	0.23 ± 0.01	1	0.3
	dG_1-C^8-IQ	C	690 ± 70	0.00022 ± 0.00001	0.0003	1
		T	460 ± 100	0.00032 ± 0.00002	0.0006	2
	dG_1-N^2-IQ	C	77 ± 11	0.0025 ± 0.00001	0.032	1
		T	100 ± 20	0.0018 ± 0.0001	0.018	0.56
pol κ	dG_1	C	68 ± 12	0.089 ± 0.005	1.3	1
		G	400 ± 50	0.0041 ± 0.0002	0.010	0.0077
	dG_1-C^8-IQ	C	360 ± 50	0.0068 ± 0.0003	0.019	1
		G	140 ± 40	0.00013 ± 0.00001	0.0009	0.047
	dG_1-N^2-IQ	C	65 ± 24	0.014 ± 0.001	0.22	1
		G	270 ± 40	0.00015 ± 0.00001	0.0005	0.0023

TABLE 3
Steady-state kinetic parameters for one-base incorporation opposite G_3 by human pols η, ι, and κ

Polymerase	Template	dNTP	K_m	k_{cat}	k_{cat}/K_m	*f* (misinsertion frequency)
			μM	s^{-1}	$mM^{-1}\,s^{-1}$	
pol η	dG_3	C	6.1 ± 0.5	0.12 ± 0.003	19.7	1
		A	230 ± 40	0.074 ± 0.004	0.32	0.016
	dG_3-C^8-IQ	C	68 ± 10	0.036 ± 0.001	0.53	1
		A	120 ± 20	0.027 ± 0.001	0.23	0.43
	dG_3-N^2-IQ	C	46 ± 9	0.11 ± 0.01	2.4	1
		A	510 ± 60	0.051 ± 0.002	0.1	0.042
pol ι	dG_3	C	42 ± 7	0.36 ± 0.01	8.6	1
		T	660 ± 50	0.37 ± 0.01	0.56	0.065
	dG_3-C^8-IQ	C	230 ± 50	0.00072 ± 0.00004	0.0031	1
		T	130 ± 20	0.0024 ± 0.0001	0.018	5.8
	dG_3-N^2-IQ	C	40 ± 8	0.0022 ± 0.00001	0.055	1
		T	50 ± 5	0.00093 ± 0.00002	0.018	0.33
pol κ	dG_3	C	79 ± 7	0.15 ± 0.005	1.9	1
		G	400 ± 50	0.0042 ± 0.0002	0.011	0.0058
	dG_3-C^8-IQ	C	320 ± 50	0.00093 ± 0.00001	0.0029	1
		G	230 ± 40	0.00006 ± 0.000003	0.0002	0.069
	dG_3-N^2-IQ	C	68 ± 21	0.011 ± 0.001	0.16	1
		G	330 ± 40	0.0024 ± 0.0001	0.0072	0.045

In the case of the sequence analysis of pol η-catalyzed full-length extension products across the C^8-IQ adduct at the G_1 position, the initial analysis was equivocal, and subsequent LC-MS/MS was performed on a Waters Acquit HPLC system (Waters, Milford, MA) connected to a Finnigan LTQ mass spectrometer (thermoelectric) using an Acuity HPLC BE C18 column (1.7 μm, 1.0 mm × 100 mm). LC conditions were as follows: buffer A contained 10 mM $NH_4CH_3CO_2$ plus 2% CH_3CN (v/v), and buffer B contained 10 mM $NH_4CH_3CO_2$ plus 95% CH_3CN (v/v). The following gradient program was used with a flow rate of 150 μl min^{-1}: 0–3 min, linear gradient from 100% A to 97% A; 3–4.5 min, linear gradient to 80% A; 4.5–5 min, linear gradient 100% B; 5–5.5 min, hold at 100% B; 5.5–6.5 min, linear gradient to 100% A; 6.5–9.5 min, hold at % A. The temperature of the column was maintained at 50 °C. Samples (10 μl) were infused with an autosampler. ES conditions were as follows: source voltage 4 kV, source current 100 μA, auxiliary gas flow rate setting 20, sweep gas flow rate setting 5, sheath gas flow setting 34, capillary voltage −49 V, capillary temperature 350 °C, tube lens voltage −90 V. MS/MS conditions were as follows: normalized collision energy 35%, activation *Q* 0.250, and activation time 30 ms. Product ion spectra were acquired over the range *m/z* 345–2000. The triply charged species (*m/z* 1152.7) were used for CID analysis. The calculations of the CID fragmentations of oligonucleotide sequences were also done using a program linked to the Mass Spectrometry Group of Medicinal Chemistry at the University of Utah.

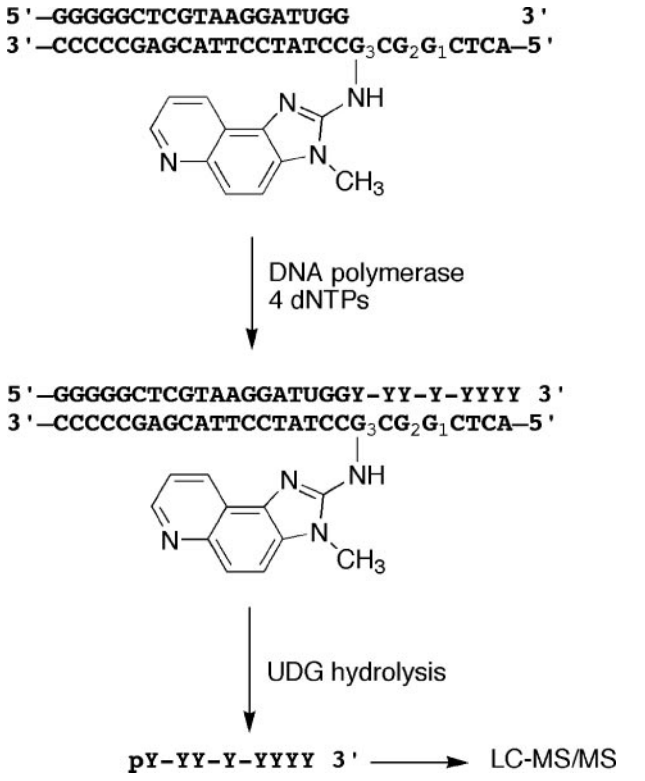

FIGURE 4. **Approach to analysis of extension products by LC-MS/MS.** The procedure involves extension of a primer beyond the G-IQ adduct in the template (C^8-IQ adduct at G_3 position in this example), digestion of the product with UDG and LC-MS/MS.

RESULTS

Extension of Primers Opposite C^8- and N^2-IQ Adducts in Templates—Initial studies were done with all four dNTPs using each of the human DNA polymerases available (δ, η, ι, and κ). Comparisons were made with the templates containing the C^8- and N^2-IQ adducts at the G_1 and G_3 positions, with the cognate primers (Figs. 2 and 3).

pol δ, in the presence of PCNA, readily extended the primers opposite the unmodified template but was totally blocked by either IQ adduct at both the G_1 or G_3 positions (Figs. 2 and 3). As expected, the translesion polymerases (η, ι, and κ) extended the primer opposite the unmodified template but with more less than full-length products due to their distributive character.

pol η extended the primer opposite the C^8-IQ adduct at the G_1 or G_3 position, although apparently better at G_1 (Fig. 2). Extension also occurred opposite the N^2-IQ adduct at both the G_1 and G_3 sites, although the products appeared to be less than full-length (Fig. 3). The latter phenomenon could be due to a lack of ability to read completely through or to deletions (see below).

Both pol ι and κ showed very limited ability to catalyze primer extension opposite the templates with the C^8- or the N^2-IQ adduct (Figs. 2 and 3). Only with the N^2-IQ adduct (both G_1 and G_3 sites) was any extension beyond a single residue seen (with pol κ) (Fig. 3).

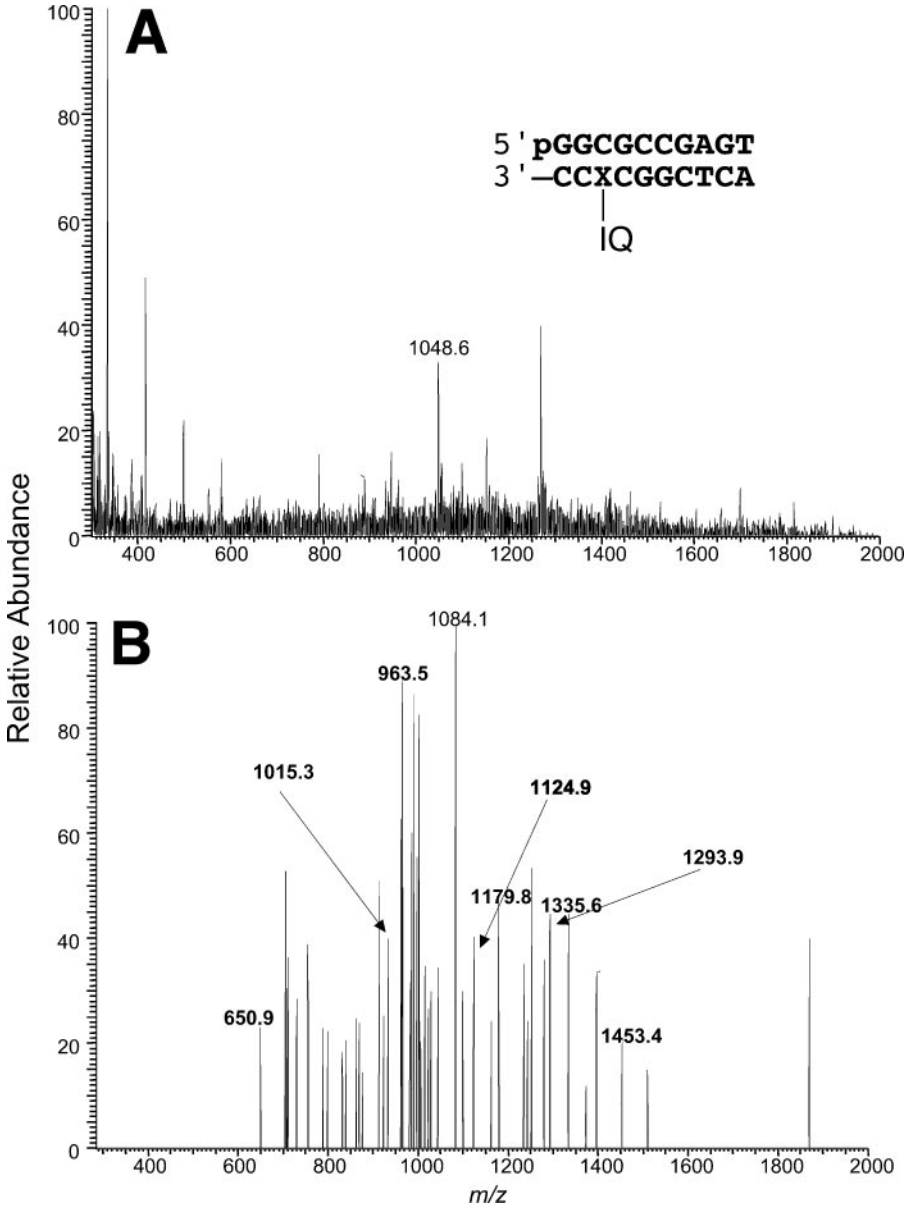

FIGURE 5. **Analysis of the pol η extension product of the primer extended opposite the template containing the C^8-IQ adduct at the G^3 site using LC-MS/MS.** *A*, mass spectrum of the oligonucleotide peak. *B*, CID mass spectrum (of the *m/z* 1048.1 ion).

Steady-state Kinetics of 1-Base Incorporation into Primers Opposite C^8- and N^2-IQ Adducts—The steady-state kinetic parameters k_{cat}, K_m, and particularly k_{cat}/K_m provide a rough quantitative estimate of the ability of polymerases to insert bases opposite an adduct. A misincorporation factor, $f\,(=(k_{cat}/K_m)_{\text{wrong dNTP}}/(k_{cat}/K_m)_{\text{dCTP}})$, provides an index of the tendency to misincorporate for comparisons (39).

Preliminary experiments indicated that the dominant incorporations opposite both the C^8- and N^2-IQ adducts were polymerase-dependent as follows: C and A for pol η, C and T for pol ι, and C and G for pol κ (Tables 1 and 2). The activity with pol δ was too low to measure (Figs. 2 and 3). The efficiencies of insertion (k_{cat}/K_m) were 1–4 orders of magnitude lower than for insertion of dCTP opposite G, depending on the particular system. dCTP insertion was preferred to other dNTPs in all but two cases ($f > 1$), both with pol ι (Tables 2 and 3). Of the various insertions (C^8- and N^2-IQ adducts at G_1 and G_3 sites), the efficiency of pol η insertion of dCTP was the most efficient for the adducts in all cases.

LC-MS/MS Analysis of Bases Inserted during Primer Extension—LC-MS/MS analysis was used to identify the extension products from the pol η reaction (with the other polymerases, the limited amounts of extended products were insufficient for any analysis). Mass spectra derived from ES ionization and CID are well suited for direct sequencing of oligonucleotides, and the method has the advantage of high sensitivity and application to modified oligonucleotides (37, 38). The same 19-mer primer used for full extension and single nucleotide insertion studies was redesigned to contain a single uracil residue (Fig. 4). Following polymerase extension of the primer positioned opposite the C^8-IQ adduct at the G_3 site in the template, the extended primers were digested by UDG followed by piperidine treatment to generate shorter oligonucleotides, which are more easily analyzed than the full-length primer product (Fig. 4). The CID spectra of longer oligonucleotide sequences are much more difficult to interpret when compared with shorter length sequences. After HPLC separation, an oligonucleotide-containing fraction was eluted at 10.55 min. Initial analysis of the ES mass spectrum indicated that *m/z* 1048.6 was the M − 3H ion (Fig. 5) and indicative of one major species present in the peak at t_R 10.55 min. CID analysis of the *m/z* 1048.6 peak is shown in Fig. 5*B*. The composition of the *m/z* 1048.6 (M-3H) oligonucleotide was 1 phosphate, 5 Gs, 3 Cs, 1 T, and 1 A. Given the composition and sequence of the template, the unknown primer extension product was determined to be 5′-pGGCGCCGAGT-3′, which is the full-length error-free bypass product (Fig. 6). The CID spectra matched well with those calculated based on the candidate sequence, with all of the major ions from Fig. 5 appearing in the calculated sequence (Table 4). The CID analysis was also compared with that of a standard oligonucleotide purchased from Midland Certified Reagent Co. (Midland, TX) (5′-pGGCGCCGAGT-3′) (shown in supplemental Fig. S5).

A similar result was observed with the C^8-IQ adduct at the G_1 position; the error-free product accounted for 95% of the extended primer. However, one additional dATP was incorpo-

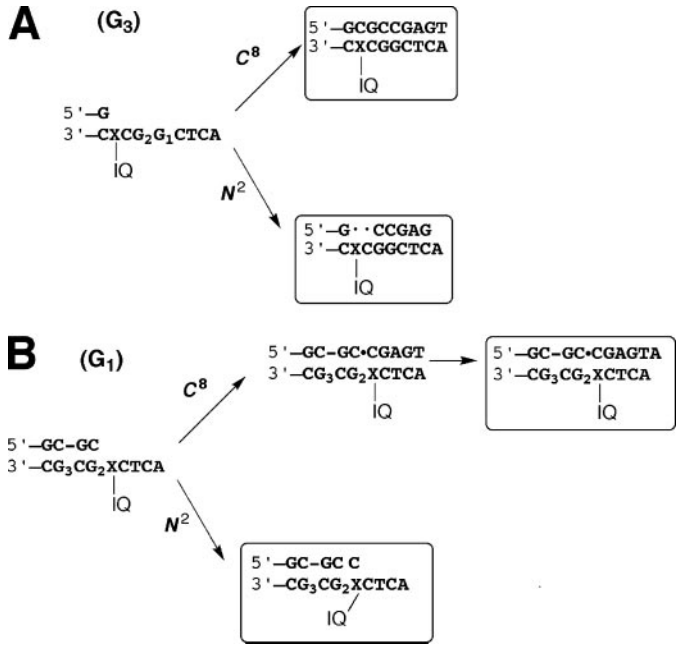

FIGURE 6. **Proposed schemes for extension of primers.** *A*, IQ adducts at the G_3 position; *B*, IQ adducts at the G_1 position.

TABLE 4

Experimental versus theoretical fragmentation for product of pol η extension experiment with C^8-IQ adduct at the G_3 site

Sequence	Experimental fragmentation[a]	Theoretical fragmentation
	m/z	*m/z*
—pGT-3′	650.9	650.1
—pAGT-3′	963.5	963.15
5′-pGGCGCCGA—	1179.89	1179.66
5′-pGGCGCCG—	1015.3	1015.14
—pGGCG-3′	1124.9	1124.14
—pGAGT-3′	1293.9	1292.20

[a] See Fig. 5.

rated at the end of the completed primer strand, in a blunt end addition (Fig. 6). These results are presented in supplemental Fig. S6.[4] An additional product (~5%) was also detected, but we have not been able to analyze the central section of the nucleotide sequence.

LC-MS/MS analysis was also used to identify the extension products past the N^2-IQ adducts of G at both positions of the NarI sequence (G_3 and G_1). Following pol η extension and UDG digestion of the primer extended opposite the N^2-IQ adduct at the G_3 site of the template, an oligonucleotide-containing peak was eluted at t_R 10.56 min during HPLC separation. Preliminary analysis of the ES mass spectrum indicated that *m/z* 1111.6 was the M − 2 ion (Fig. 7), indicating one major species present in the peak at 10.56 min. The possible composition of the *m/z* 1111.6 (M − 2H) oligonucleotide was 1 phosphate, 4 Gs, 2 Cs, and 1 A. Given the composition and sequence of the template, the unknown primer extension product was determined to be 5′-pGGCCGAG-3′, a −2 deletion product (Fig. 6). CID analysis of the *m/z* 1111.6 peak is shown in Fig. 7. The CID spectra matched well with those calculated based on the candidate sequence, with all of the major ions from Fig. 7 appearing in the calculated sequence (Table 5). The CID analysis was also compared with that obtained for a standard commercial oligonucleotide (Midland) (5′-pGGCCGAG-3′) and is shown in Fig. 8.

The same LC-MS/MS analysis was carried out for the oligonucleotide primer extended opposite the N^2-IQ adduct at the G_1 site (supplemental Fig. S7). The major extension product was a blocked one, 5′-pGGCGCC-3′, in which the polymerase was unable to process to the end of the sequence. The LC-MS/MS results indicated that only C was inserted in the primer extension product that was analyzed (Fig. 6). However, steady-state kinetic analysis had indicated that pol η inserted both dCTP and dATP opposite the G_1 position N^2-IQ G adduct, with nearly equal efficiency (Table 2). In light of this apparent discrepancy, we examined the further extension of a primer with A inserted opposite the G_1 N^2-IQ adduct and found no activity (supplemental Fig. S8). Thus, we conclude that both C and A can be inserted but that pol η extends only beyond the N^2-IQ G:C pair.

DISCUSSION

One of the most interesting aspects of the heterocyclic amines is their extremely high mutagenicity (8, 9, 13). Most reports have focused on bacterial systems; the weaker mutagenicity seen in some mammalian cells has been attributed to the lack of the relevant bioactivation systems (40). In this work, we positioned both the N^2- and C^8-IQ adducts at both the G_1 and G_3 sites in the NarI sequence. In all cases, no replication of a primer occurred with human pol δ, even in the presence of PCNA, but the translesion polymerases pol η, ι, and κ could achieve some bypass. Of these, pol η was clearly the most efficient (Tables 1 and 2). The steady-state kinetic analysis suggested that dCTP insertion was favored in all cases, indicative of fidelity. However, LC-MS/MS analysis of the pol η primer extension products indicated that one of the four cases produced a frameshift mutation, with the N^2-IQ adduct showing the common NarI CG/GC deletion only at the G_3 position. Of the four cases, only the two C^8-IQ adducts showed fidelity of replication. These *in vitro* results support the high inherent mutagenicity of IQ adducts and also show the major differences among individual chemistry of modifications, as well as with regard to the DNA site and individual polymerases.

Fuchs *et al.* (17) first reported that treatment of bacteria with *N*-acetoxy-AAF resulted in mutation at a hot spot, yielding a prominent −2 (GC) deletion in the center of a NarI site (GGCGCC). All three guanines in this sequence showed similar levels of adduction, but the G_3 site was most "mutation-prone" (18). Subsequently, the same group was able to prepare plasmids in which each of the three guanines in the NarI sequence had been modified with (*N*-acetoxy) AAF (41), and only the G_3 position yielded the −2 deletion (19). The Fuchs laboratory also demonstrated that IQ caused similar −1 and −2 deletions (42). The IQ-induced deletions were reported to be SOS-independent, in contrast to those seen with AAF, which seems surprising in light of the current knowledge about translesion synthesis (1, 4, 5). The −1 deletions induced by AAF have also been

[4] This is the same major product that resulted from polymerization past the N^2-IQ adduct placed at the G_3 site by *Sulfolobus solfataricus* DNA polymerase Dpo4 (J. S. Stover, H. Zang, G. Chowdhury, F. P. Guengerich, and C. J. Rizzo, submitted for publication).

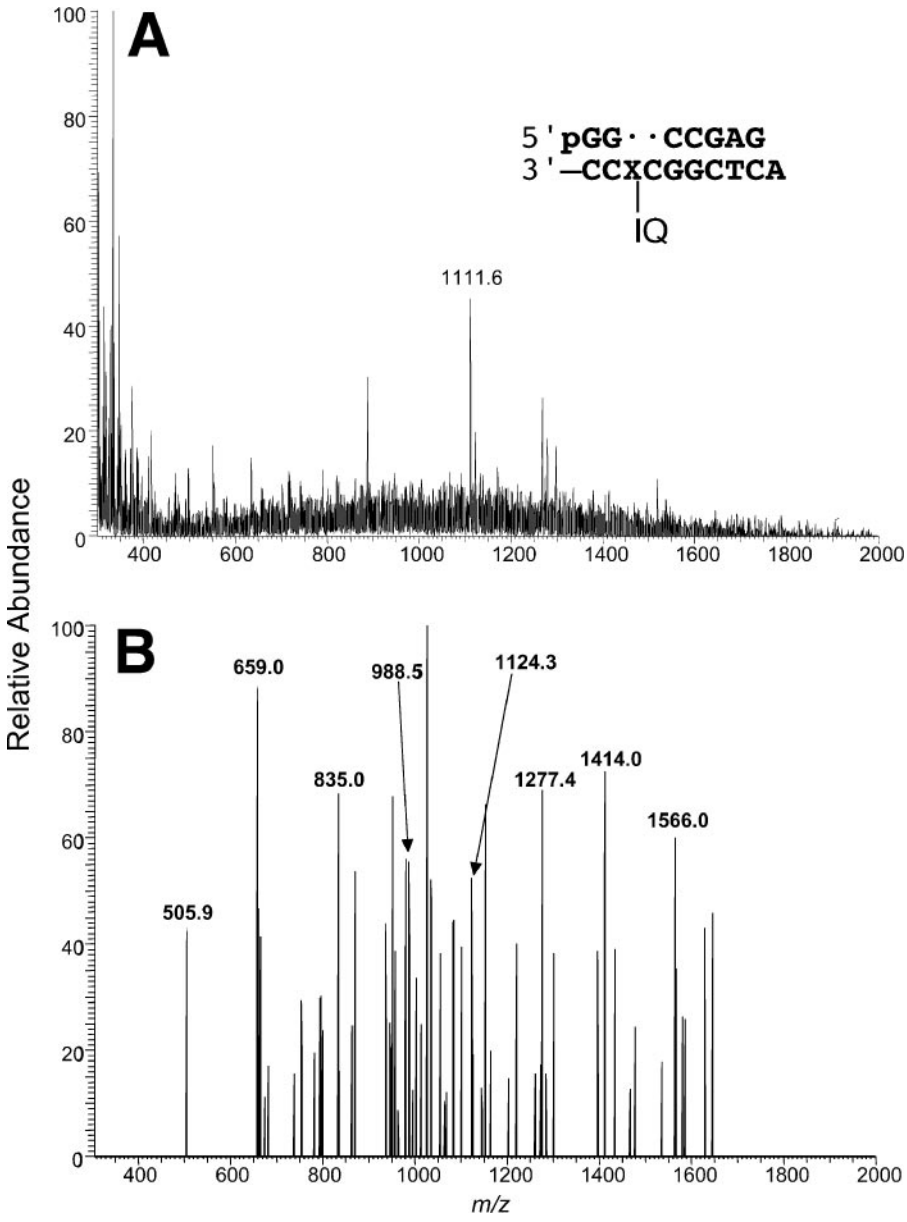

FIGURE 7. **Analysis of the pol η extension product of the primer extended opposite the template containing the N^2-IQ adduct at the G_3 site using LC-MS/MS.** *A*, mass spectrum of the oligonucleotide peak. *B*, CID mass spectrum (of the *m/z* 1111.6 ion).

TABLE 5

Experimental versus theoretical fragmentation for product of pol η extension experiment with N^2-IQ adduct at the G_3 site

Sequence	Experimental fragmentation[a]	Theoretical fragmentation
	m/z	*m/z*
—pAG-3′	659.1	659.11
—pGAG-3′	988.5	988.16
5′-pGGC—	835.0	835.09
5′-pGGCCG—	1414.1	1413.19
—pCCGAG-3′	1566.1	1566.25
—pCGAG-3′	1277.5	1277.20

[a] See Figs. 7 and 8.

studied in runs of guanines and proposed to be the result of a slippage mechanism (43). Other subsequent work confirmed that the modification of G_3 guanine of the NarI sequence with AAF produced an SOS-dependent frameshift in *E. coli* (23). The AF adduct at the same site produced only G to T transversions (in *E. coli*), and both AF and AAF produced G to T transversions in COS-7 kidney cells. Similar findings regarding G_3 −2 deletions (in an *E. coli* system) for AAF G_3 site adduct(s) were reported by Tebbs and Romano (29).

Attempts to understand the molecular basis of the −2 deletions have been made. Burnouf *et al.* (44) used AAF-modified oligonucleotides with several DNA polymerases (*E. coli* polymerase I (Klenow fragment, + or − exonuclease), bacteriophage T7 polymerase, *E. coli* pol III α subunit, and pol III holoenzyme). A variety of results was found, depending upon the polymerase. The G_1 adduct (AAF) produced error-free replication, and the G_2 and G_3 sites yielded mutations. However, none of these polymerases produced the GC deletions. Gill and Romano (20), in contrast, reported that Klenow fragment (exonuclease$^-$) produced a GC deletion when copying the NarI sequence with an AAF adduct at G_3 but did not provide specific evidence. Crystal structures of two replicative DNA polymerases bound to AAF-modified DNA have been solved, with *Bacillus stearothermophilus* pol I (45) and bacteriophage pol T7 (46). AF-adducted G appears to pair with C; in both reports the C^8-G AAF adduct induces an *anti* to *syn* shift in the glycosidic bond, which in the case of pol T7 leads to intercalation of the AAF fluorene ring into the hydrophobic pocket of the polymerase and locks it in the "open" conformation (46).

Less information is available to date about IQ adducts than AAF. As mentioned earlier, the guanine C^8-IQ adduct is formed more readily in DNA than the N^2-IQ adduct, but the N^2-IQ accumulates *in vivo* due to slower repair (27, 28). IQ is mutagenic in human lymphoblastoid cells, but the limited mutation is probably the result of deficient bioactivation (40). The point should also be raised that there is a rather limited knowledge of which translesion DNA polymerases are present in various cell lines, which may be important (Fig. 1 and Tables 1 and 2). A −2 deletion (−GC) is a prominent mutation observed in transgenic (+*lac*) rats (liver, colon, and kidney) (30). Another heterocyclic amine adduct, the C^8-guanyl derivative of 2-amino-1-methyl-6-phenylimidazo[4,5-*b*]pyridine (commonly referred to as "PhIP"), has been examined in *E. coli* and COS-7 cells (47); G to

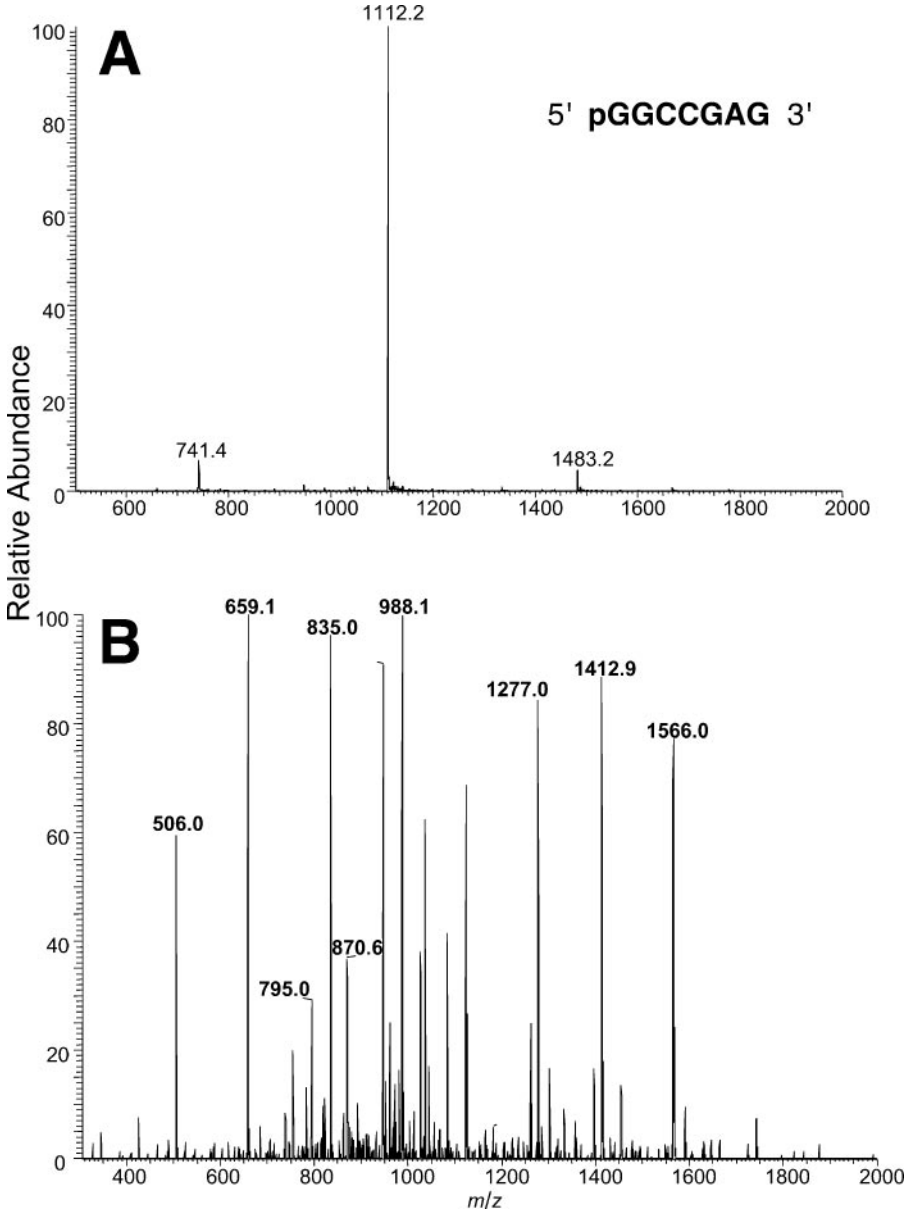

FIGURE 8. **MS of synthesized 5′-pGGCCGAG-3′.** The synthetic oligonucleotide was used to confirm the assignment of the product identified in the primer extension opposite to the N^2-IQ adduct at the G_3 template site (Fig. 7). *A,* mass spectrum; *B,* CID spectrum (of the *m/z* 1112.2 ion).

T transversions and −1 deletions were observed, but the results were variable depending upon the sequence context.

In our work presented here, the GC (2-base) deletion was restricted to the N^2-IQ adduct at the G_3 site of the NarI sequence (Fig. 4) and was only really seen with pol η. The single-base insertion steady-state results (preferential insertion of dCTP) are misleading in that this is in all likelihood not a direct insertion opposite the modified G but rather opposite the G two bases 5′ of the adduct. These findings with pol η may provide some potential insight into the −2 deletion seen *in vivo* in rats (30).

pol κ is able to bypass bulky lesions such as those formed from benzo[*a*]pyrene diol epoxide (48–51), although the kinetic parameters are difficult to compare in these cited studies because of the expression of units, and furthermore, sequence contexts can influence the outcomes (51). A role for pol κ has been suggested for bypass of AAF C^8-G adducts (52). However, in the context used, the conclusion was that (a truncated form of) pol κ inserted dTTP opposite the AAF adduct (52). In our own work with the IQ adducts (Tables 2 and 3), pol η was considerably more active than pol κ. With some systems a two-step process has been invoked in which pol ηcopies opposite lesions and then pol κ proceeds to extend (48, 50, 53, 54). In the present work with the IQ adducts, pol η could extend past the adducts without pol κ (Figs. 2 and 3). Accordingly, we did not use mixtures of the polymerases in our work, which would have obfuscated quantitative measurements (Tables 2 and 3) and also the interpretation of LC-MS/MS analysis of products in the context of individual enzymes.

The NarI system has been used as a model for development of a system for studying the DNA site specificity of heterocyclic amine mutagenesis *in vitro*. However, some of the findings with the IQ adducts may not be directly relevant to the results obtained with AAF and vice versa. In addition, one concern about much of the earlier work with AAF is the identity of the adducts. Although the C^8-guanyl adduct is the most plentiful in the treatment of DNA with *N*-hydroxy-IQ (27) or *N*-acetoxy-AAF (55, 56), some N^2-guanyl adduct is formed, and oligonucleotides substituted with C^8- and N^2-guanyl adducts might not be readily discerned except with careful UV or MS CID analysis. The difference in the course of the primer extensions of the C^8- and N^2-IQ G_3 adducts is remarkable (Fig. 4), and the possibility exists in a biological experiment (*i.e.* mutagenesis) that a trace of N^2(−AAF) adduct might be responsible for activities attributed to the C^8 adduct. For further understanding of IQ mutagenesis, one important need is analysis of x-ray structures of polymerases bound to IQ-modified oligonucleotides. Another need in this area is cellular analysis of which DNA polymerases are involved in translesion bypass and mutagenesis. Although the evidence presented here supports a role of pol η, the analysis does not include all of the DNA polymerases potentially involved. Furthermore, the expression of the individual mammalian translesion DNA polymerases in various cell lines and tissues (*in vivo*) is not well characterized.

In conclusion, we have been able to show that IQ-dependent mutations are functions of the adduct chemistry, the DNA loca-

tion, and the individual DNA polymerase involved. Although the literature already contains information for this general view with other types of DNA adducts, the point is clearly shown here with the altered adduct chemistry and with three of the major human translesion DNA polymerases. We have been able to dissect a mutagenic signature shown in mammals (a −2 base GC deletion) into components associated with different polymerases and sites. There are caveats about comparing human DNA polymerases with results in rats, but any comparisons with cells of human origin in culture have their own deficiencies. These results demonstrate a source of 2-base deletions provides a basis for further structural and biological experiments involving mechanisms and relevance.

Acknowledgments—We thank M. L. Manier for assistance with LC-MS/MS and K. Trisler for assistance in preparation of the manuscript.

REFERENCES

1. Friedberg, E. C., Walker, G. C., Siede, W., Wood, R. D., Schultz, R. A., and Ellenberger, T. (2006) *DNA Repair and Mutagenesis*, 2nd Ed., American Society for Microbiology, Washington, D. C.
2. Ramos, K. S., and Moorthy, B. (2005) *Drug Metab. Rev.* **37,** 595–610
3. Guengerich, F. P. (2006) *Chem. Rev.* **106,** 420–452
4. Prakash, S., Johnson, R. E., and Prakash, L. (2005) *Annu. Rev. Biochem.* **74,** 317–353
5. Goodman, M. F. (2002) *Annu. Rev. Biochem.* **71,** 17–50
6. Kunkel, T. A. (2004) *J. Biol. Chem.* **279,** 16895–16898
7. Valadez, J. G., and Guengerich, F. P. (2004) *J. Biol. Chem.* **279,** 13435–13446
8. Sugimura, T. (1997) *Mutat. Res.* **376,** 211–219
9. Turesky, R. J. (2002) *Drug Metab. Rev.* **34,** 625–650
10. Kim, D., and Guengerich, F. P. (2005) *Annu. Rev. Pharmacol. Toxicol.* **45,** 27–49
11. Wogan, G. N., Hecht, S. S., Felton, J. S., Conney, A. H., and Loeb, L. A. (2004) *Semin. Cancer Biol.* **14,** 473–486
12. Felton, J. S., and Knize, M. G. (1990) *Prog. Clin. Biol. Res.* **347,** 19–38
13. Nagao, M., Honda, M., Seino, Y., Yahagi, T., and Sugimura, T. (1977) *Cancer Lett.* **2,** 221–226
14. Rehn, L. (1895) *Arch. Clin. Chirgurie* **50,** 588–600
15. Beland, F. A., and Kadlubar, F. F. (1985) *Environ. Health Perspect.* **62,** 19–30
16. Adamson, R. H. (2000) in *Food Borne Carcinogens Heterocyclic Amines* (Nagao, M., and Sugimura, T., eds) pp. 229–240, John Wiley & Sons Ltd., Chichester, UK
17. Fuchs, R. P., Schwartz, N., and Daune, M. P. (1981) *Nature* **294,** 657–659
18. Koffel-Schwartz, N., Verdier, J. M., Bichara, M., Freund, A. M., Daune, M. P., and Fuchs, R. P. (1984) *J. Mol. Biol.* **177,** 33–51
19. Burnouf, D., Koehl, P., and Fuchs, R. P. P. (1989) *Proc. Natl. Acad. Sci. U. S. A.* **86,** 4147–4151
20. Gill, J. P., and Romano, L. J. (2005) *Biochemistry* **44,** 15387–15395
21. Mao, B., Gu, Z., Gorin, A., Hingerty, B. E., Broyde, S., and Patel, D. J. (1997) *Biochemistry* **36,** 14491–14501
22. Cho, B. P., and Zhou, L. (1999) *Biochemistry* **38,** 7572–7583
23. Tan, X., Suzuki, N., Grollman, A. P., and Shibutani, S. (2002) *Biochemistry* **41,** 14255–14262
24. Elmquist, C. E., Stover, J. S., Wang, Z., and Rizzo, C. J. (2004) *J. Am. Chem. Soc.* **126,** 11189–11201
25. Stover, J. S., and Rizzo, C. J. (2004) *Org. Lett.* **6,** 4985–4988
26. Wang, Z., and Rizzo, C. J. (2001) *Org. Lett.* **3,** 565–568
27. Turesky, R. J., and Vouros, P. (2004) *J. Chromatogr. B* **802,** 155–166
28. Turesky, R. J., Box, R. M., Markovic, J., Gremaud, E., and Snyderwine, E. G. (1997) *Mutat. Res.* **376,** 235–241
29. Tebbs, R. S., and Romano, L. J. (1994) *Biochemistry* **33,** 8998–9006
30. Bol, S. A. M., Horlbeck, J., Markovic, J., de Boer, J. G., Turesky, R. J., and Constable, A. (2000) *Carcinogenesis* **21,** 1–6
31. Choi, J.-Y., and Guengerich, F. P. (2005) *J. Mol. Biol.* **352,** 72–90
32. Choi, J.-Y., and Guengerich, F. P. (2006) *J. Biol. Chem.* **281,** 12315–12324
33. Choi, J.-Y., Angel, K. C., and Guengerich, F. P. (2006) *J. Biol. Chem.* **281,** 21062–21072
34. Fien, K., and Stillman, B. (1992) *Mol. Cell Biol.* **12,** 155–163
35. Einolf, H. J., and Guengerich, F. P. (2000) *J. Biol. Chem.* **275,** 16316–16322
36. Tretyakova, N., Matter, B., Ogdie, A., Wishnok, J. S., and Tannenbaum, S. R. (2001) *Chem. Res. Toxicol.* **14,** 1058–1070
37. Ni, J., Pomerantz, S. C., Rozenski, J., Zhang, Y., and McCloskey, J. A. (1996) *Anal. Chem.* **68,** 1989–1999
38. Zang, H., Goodenough, A. K., Choi, J.-Y., Irminia, A., Loukachevitch, L. V., Kozekov, I. D., Angel, K. C., Rizzo, C. J., Egli, M., and Guengerich, F. P. (2005) *J. Biol. Chem.* **280,** 29750–29764
39. Boosalis, M. S., Petruska, J., and Goodman, M. F. (1987) *J. Biol. Chem.* **262,** 14689–14696
40. Leong-Morgenthaler, P. M., Velt, C. O. H., Jaccaud, E., and Turesky, R. J. (1998) *Carcinogenesis* **19,** 1749–1754
41. Koehl, P., Burnouf, D., and Fuchs, R. P. P. (1989) *J. Mol. Biol.* **207,** 355–364
42. Maenhaut-Michel, G., Janel-Bintz, R., Samuel, N., and Fuchs, R. P. (1997) *Mol. Gen. Genet.* **253,** 634–641
43. Napolitano, R. L., Lambert, I. B., and Fuchs, R. P. P. (1994) *Biochemistry* **33,** 1311–1315
44. Burnouf, D. Y., Miturski, R., and Fuchs, R. P. (1999) *Chem. Res. Toxicol.* **12,** 144–150
45. Hsu, G. W., Kiefer, J. R., Burnouf, D., Becherel, O. J., Fuchs, R. P., and Beese, L. S. (2004) *J. Biol. Chem.* **279,** 50280–50285
46. Dutta, S., Li, Y., Johnson, D., Dzantiev, L., Richardson, C. C., Romano, L. J., and Ellenberger, T. (2004) *Proc. Natl. Acad. Sci. U. S. A.* **101,** 16186–16191
47. Shibutani, S., Fernandes, A., Suzuki, N., Zhou, L., Johnson, F., and Grollman, A. P. (1999) *J. Biol. Chem.* **274,** 27433–27438
48. Zhang, Y., Wu, X., Guo, D., Rechkoblit, O., and Wang, Z. (2002) *DNA Repair* **1,** 559–569
49. Rechkoblit, O., Zhang, Y., Guo, D., Wang, Z., Amin, S., Krzeminsky, J., Louneva, N., and Geacintov, N. E. (2002) *J. Biol. Chem.* **277,** 30488–30494
50. Zhang, Y., Wu, X., Guo, D., Rechkoblit, O., Geacintov, N. E., and Wang, Z. (2002) *Mutat. Res.* **510,** 23–35
51. Huang, X., Kolbanovskiy, A., Wu, X., Zhang, Y., Wang, Z., Zhuang, P., Amin, S., and Geacintov, N. E. (2003) *Biochemistry* **42,** 2456–2466
52. Suzuki, N., Ohashi, E., Hayashi, K., Ohmori, H., Grollman, A. P., and Shibutani, S. (2001) *Biochemistry* **40,** 15176–15183
53. Washington, M. T., Johnson, R. E., Prakash, L., and Prakash, S. (2002) *Proc. Natl. Acad. Sci. U. S. A.* **99,** 1910–1914
54. Haracska, L., Prakash, L., and Prakash, S. (2002) *Proc. Natl. Acad. Sci. U. S. A.* **99,** 16000–16005
55. Miller, E. C., Juhl, U., and Miller, J. A. (1966) *Science* **153,** 1125–1127
56. Novak, M., and Kennedy, S. A. (1995) *J. Am. Chem. Soc.* **117,** 574–575

Biochemical Basis of Genotoxicity of Heterocyclic Arylamine Food Mutagens: HUMAN DNA POLYMERASE η SELECTIVELY PRODUCES A TWO-BASE DELETION IN COPYING THE N2-GUANYL ADDUCT OF 2-AMINO-3-METHYLIMIDAZO[4,5-f]QUINOLINE BUT NOT THE C8 ADDUCT AT THE NarI G3 SITE

Jeong-Yun Choi, James S. Stover, Karen C. Angel, Goutam Chowdhury, Carmelo J. Rizzo and F. Peter Guengerich

J. Biol. Chem. 2006, 281:25297-25306.
doi: 10.1074/jbc.M605699200 originally published online July 10, 2006
